

Synthesis and performance of a thermosetting resin: Acrylated epoxidized soybean oil curing with a rosin-based acrylamide

Yanping Yang,¹ Minggui Shen,^{1,2} Xin Huang,^{1,2} Haibo Zhang,¹ Shibin Shang,^{1,2} Jie Song³

¹Institute of Chemical Industry of Forestry Products, Chinese Academy of Forestry, Key Laboratory of Biomass Energy and Material, National Engineering Laboratory for Biomass Chemical Utilization, Key Laboratory on Forest Chemical Engineering, State Forestry Administration, Nanjing 210042 Jiangsu Province, China

²Institute of New Technology of Forestry, Chinese Academy of Forestry, Beijing 100091, China

³Department of Chemistry and Biochemistry, University of Michigan-Flint, Flint Michigan 48502

Correspondence to: S. Shang (E-mail: shangsb@hotmail.com)

ABSTRACT: A synthesized rosin-based polymeric monomer, *N*-dehydroabiatic acrylamide (DHA-AM), was introduced into an acrylated epoxidized soybean oil (AESO)/DHA-AM system to afford a thermosetting resin through thermocuring. Different molar ratios of the thermosetting AESO/DHA-AM samples were obtained through curing in the presence of an initiator, and the curing processes of the AESO/DHA-AM systems were evaluated by differential scanning calorimetry. The structures and performances of the resulting thermosets were characterized by Fourier transform infrared spectroscopy, dynamic mechanical analysis, elemental analysis, thermogravimetric analysis, and contact angle (θ) analysis. The analyses showed that with increasing content of DHA-AM introduced into the copolymer, the storage modulus, glass-transition temperature, thermal stability, and θ values of the cured samples all increased. Moreover, the copolymers changed from hydrophilic materials to hydrophobic materials. The results also demonstrate that the rosin acid derivatives showed comparable properties to those of reported petroleum-based rigid compounds for the preparation of soybean-oil-based thermosets. The presence of DHA-AM moieties in the composite structures could expand the use of AESO into the development of heat-resistant and hydrophobic materials. © 2016 Wiley Periodicals, Inc. *J. Appl. Polym. Sci.* **2017**, *134*, 44545.

KEYWORDS: crosslinking; mechanical properties; thermogravimetric analysis (TGA); thermosets

Received 14 July 2016; accepted 5 October 2016

DOI: 10.1002/app.44545

INTRODUCTION

With the lack of conventional fossil fuels and the aggravation of environmental pollution, the attraction to biomass sources, such as rosin, cellulose, starch, and vegetable oil, is increasing.¹ As one of the most abundant renewable vegetable oils, soybean oil contains double bonds, which can be used in many reactions.² Epoxidized soybean oil, the primary modified product of natural soybean oil, is obtained through the epoxidation reaction with soybean oil.³ With characteristics of little irritation and a low viscosity, epoxidized soybean oil is widely used in the areas of plasticizers, food packaging materials, pharmaceutical products, and so on.^{4,5} The further derived acrylated epoxidized soybean oil (AESO; see Figure 1), which contains reactive vinyl groups, has been applied in the areas of coatings, packaging materials, paints, and adhesives.^{6–10} Although it has other advantages, such as a low toxicity and inherent biodegradability, the inferior glass-transition temperature (T_g), mechanical

properties, and weak rigidity of AESO limits its application prospects in structural applications because of its aliphatic structure.¹¹

For the sake of improving these relatively poor properties, a rigid polymeric monomer performing as a copolymer has been introduced into the polymerization system to enhance its T_g , rigidity, and mechanical properties. For example, reactive diluents were blended with AESO to improve its unfavorable properties.^{12,13} Coincidentally, vinyl ester resin, which contains stiff aromatic units, was copolymerized with AESO to form a possible interpenetrating network structure.¹⁴ Furthermore, acting as the rigid components, petroleum-based products such as styrene,^{15,16} divinylbenzene,^{17–20} dicyclopentadiene, norbornadiene,²¹ and acrylated epoxidized fatty methyl ester²² have been introduced into AESO.

Rosin, an important natural resource that contains a three-phenanthrene-ring skeleton, is obtained by the heating of fresh

Additional Supporting Information may be found in the online version of this article.

© 2016 Wiley Periodicals, Inc.

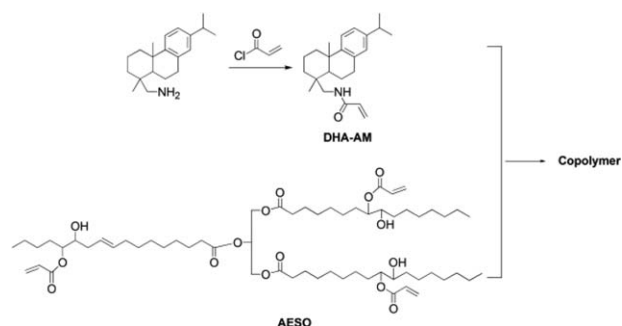


Figure 1. Scheme for the copolymerization of the AESO/DHA-AM system.

resins to eliminate volatile terpene components from pines and other plants (e.g., conifers).²³ The modified products of rosin are manifold, and they have been used in paper sizing, printing inks, and adhesives.²⁴ On the other hand, polymerized rosin derivatives are important parts of modified rosin products. Rosin-based polymers, including epoxy resin,²⁵ polyester, polyamide, and polyimide, have been investigated extensively by researchers.²⁶ Vinyl, acrylate, and allyl ester based rosin polymeric monomers acting as free-radical-chain polymeric monomers are the main modified rosin products that are used widely in paints, curing agents, and resins.²⁷ Rosin-based polymeric monomers contain polyimide,²⁸ or polyamide units make the polymers display good mechanical properties, wear resistance, and heat resistance. Hence, it has been given much attention by researchers.^{29,30} Ma *et al.*³¹ prepared a full bio-based thermosetting resin from soybean oil and rosin derivatives. The rosin derivatives showed great potential for replacing petroleum-based rigid compounds in the synthesis of bio-based thermosets with satisfactory properties. To achieve the necessary rigidity and improve the strength of bio-based thermosetting resins for some end-use applications,³² we designed and synthesized a rosin-based polymeric monomer, *N*-dehydroabietyl acrylamide (DHA-AM), with a polymeric double-bond structure and an amide unit in the monomer. The homopolymer of the synthesized monomer appeared to have good thermal stability and a high T_g .³³

In this study, synthesized DHA-AM was blended with AESO to prepare a thermosetting resin by thermocuring. Fourier transform infrared (FTIR) spectroscopy, differential scanning calorimetry (DSC), thermogravimetric analysis (TGA), dynamic mechanical analysis (DMA), and contact angle (θ) testing were used to characterize the structure and properties of the polymers. With increasing content of DHA-AM introduced in the copolymer, the storage modulus (E'), T_g , and thermal stability of the cured samples all increased. As reported, the breaking elongation of AESO/DHA-AM40 (AESO/DHA-AM = 60:40 mol/mol) increased to 36.1%, which was higher than the breaking elongation of AESO/rosin derivative copolymers (13.9%) reported in the literature.³¹ The hydrogen bonding in our synthesized DHA-AM played a necessary role in the breaking elongation value in the copolymer.

EXPERIMENTAL

Materials

Dehydroabietylamine was provided by Hangzhou Wanjing New Materials Co., Ltd. (China). Acryloyl chloride (96%, with 200-

ppm MEHQ as a stabilizer) and *tert*-butyl peroxybenzoate (96%) were purchased from Aladdin Reagent Co., Ltd. (Shanghai, China). Dichloromethane (CH₂Cl₂; 99.5%), hydrochloric acid (HCl; 37%), potassium carbonate (K₂CO₃; 99%), and sodium chloride (NaCl; 99.5%) were all offered by Chinese Medicine Group Chemical Reagent Co., Ltd. (China).

Preparation of the Rosin-Based Monomer (DHA-AM)

DHA-AM was prepared according to a procedure described in our previously published article, and the characterization is provided in the Supporting Information.³³ Acryloyl chloride (8.145 g, 0.09 mol) was dissolved in 50 mL of dried CH₂Cl₂. Then, the mixture was added to a 250-mL, three-necked flask with a magnetic stirrer, thermometer, and reflux condenser. The solution was cooled to -5°C and was stable for a while at this temperature. Subsequently, a solution of dehydroabietylamine (17.128 g, 0.06 mol) in dried CH₂Cl₂ (50 mL) was added dropwise into the cooled acryloyl chloride solution over 30 min. After that, the temperature was elevated to 23°C , and the reaction was continued for 30 min. The resulting mixture was washed successively with diluted HCl, saturated K₂CO₃ solution, and distilled water. A final white solid was obtained as the product after the residual solvent was removed by vacuum distillation.

Curing Process of AESO and DHA-AM

AESO and DHA-AM were added to a three-necked flask with different molar ratios (in Table I). After the dissolution of DHA-AM in AESO, 2% initiator *tert*-butyl benzoyl peroxide was added to the flask. When the addition was finished, the mixture was stirred vigorously until a homogeneous system was obtained. Until all of the preparation was finished, the reaction media was then poured into a mold and reacted at the curing temperature for 4 h (the temperature according to the DSC exothermic curves is listed in Table I); it was then reacted at 170°C for 5 h. To prevent cracking, the cured samples were cooled to room temperature slowly after the curing reaction.

Purification of the Cured Sample

CH₂Cl₂ (500 mL) was added to a 1000-mL, round-bottomed flask equipped with a Soxhlet extractor, and 1 g of the cured sample was added. After 40 h of refluxing, the resulting samples were removed and dried for 8 h in a vacuum oven before further characterization.

Characterization

FTIR spectra were obtained with an IS10 FTIR instrument (Nicolet) for the attenuation total reflection test. DSC was recorded with a DSC 8000 instrument (PerkinElmer) with a 3–4-mg sample at a nitrogen flow rate of 50 mL/min and temperatures from 60 to 250°C with a heating rate of $10^\circ\text{C}/\text{min}$. DMA was performed on a Q800 dynamic mechanical analyzer (TA Instruments) in three-point bending mode. The temperature of the sample with a size of $20 \times 15 \times 2 \text{ mm}^3$ was ramped from -10 to 120°C at a heating rate of $2^\circ\text{C}/\text{min}$ and a frequency of 1 Hz. The mechanical properties of the cured resins were evaluated on a universal testing machine CMT 6503 (Shenzhen SANS Test Machine Co., Ltd., China) at a crosshead speed of 10 mm/min, and the average value of at least five replicates for each sample was obtained. All of the testing samples were processed with a support span of 50 mm according to ASTM D

Table I. Compositions and Curing Temperatures of the Different Samples

Sample	Molar ratio (%)		T_{\max} (°C)	Curing temperature (°C)	Postcuring temperature (°C)
	AESO	DHA-AM			
AESO/DHA-AM0	100	0	135	110	170
AESO/DHA-AM10	90	10	144	120	170
AESO/DHA-AM20	80	20	151	130	170
AESO/DHA-AM30	70	30	153	130	170
AESO/DHA-AM40	60	40	156	130	170

638-03. All of the samples were tested at 25 °C. TGA was done with a 409PC thermogravimetric analyzer. Each of samples was tested from 35 to 700 °C at a heating rate of 15 °C/min under a nitrogen atmosphere. The hydrophobic characteristics of the cured samples were determined with a Kruss tensiometer (Easy Drop DSA-2). The sessile drop method, in which drops were created with a syringe, was used to test the θ s. The θ of each sample was determined with 3–5 μ L of distilled water dropped on the surface of the samples. After three tests, the average was taken.

RESULTS AND DISCUSSION

Thermal Curing Behavior of Different Proportions of AESO/DHA-AM

To investigate the curing behavior of the different proportions of AESO/DHA-AM, scanning curing exotherms of these cured samples were obtained from the DSC measurements. Images of the scanning curing exotherms are shown in Figure 2, and the results are summarized in Table I. The results suggest that only a large exothermic peak appeared in the curves of all of the proportions of AESO/DHA-AM. The curing exothermic starting temperature and the exothermic peak temperature (T_{\max}) all grew after the addition of the rosin-based monomer. When more DHA-AM was added, the curing exothermic starting temperature and T_{\max} were higher. To our knowledge, the curing exothermic starting temperature and T_{\max} had direct relationships with the reactivity of the component.^{31,34} When the

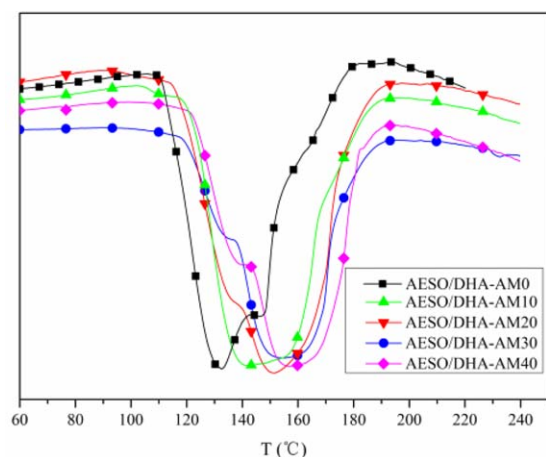


Figure 2. DSC thermograms of the curing procedure with different AESO/DHA-AM contents. [Color figure can be viewed at wileyonlinelibrary.com]

curing exothermic starting temperature and T_{\max} of the curing process were higher, the reactivity of the component was lower. Obviously, the curing exothermic starting temperature of AESO/DHA-AM0 was about 110 °C, and T_{\max} was about 135 °C; these values were lower than those of AESO/DHA-AM systems with other proportions during the polymerization. With increasing DHA-AM content, the curing exothermic starting temperature and T_{\max} were elevated. This result shows that with the addition of DHA-AM, the reactivity of the component was lower than that of the single AESO system; this was due to the lower reactive vinyl electron density in the AESO/DHA-AM systems compared to that in the single AESO system.

FTIR Spectra of the AESO and Cured Samples

Figure 3 shows FTIR spectra of the monomers and cured samples, in which the C=O bond in AESO and cured samples was confirmed by the characteristic peak at 1735 cm^{-1} . The C=O bond at 1656 cm^{-1} was found in DHA-AM because of its conjugation with N—H. Characteristic absorptions for C=C were detected at 1623 and 1638 cm^{-1} , respectively, in AESO. The peak at 1623 cm^{-1} was formed because of the conjugation between C=C and C=O in AESO. However, in the cured samples, the characteristic absorption for the C=C stretching

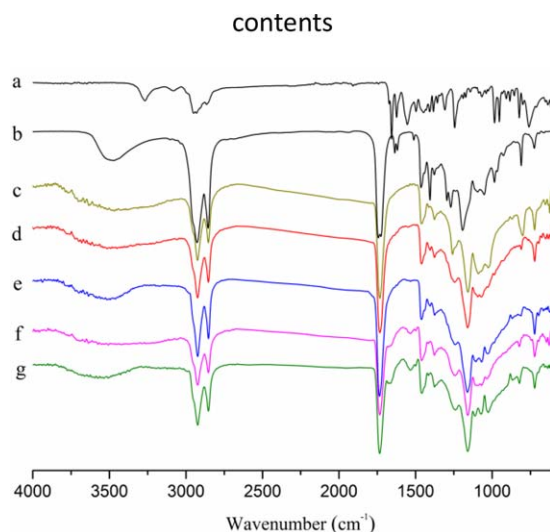


Figure 3. FTIR spectra of the monomers and cured samples: (a) DHA-AM monomer, (b) AESO monomer, (c) AESO/DHA-AM0, (d) AESO/DHA-AM10, (e) AESO/DHA-AM20, (f) AESO/DHA-AM30, and (g) AESO/DHA-AM40. [Color figure can be viewed at wileyonlinelibrary.com]

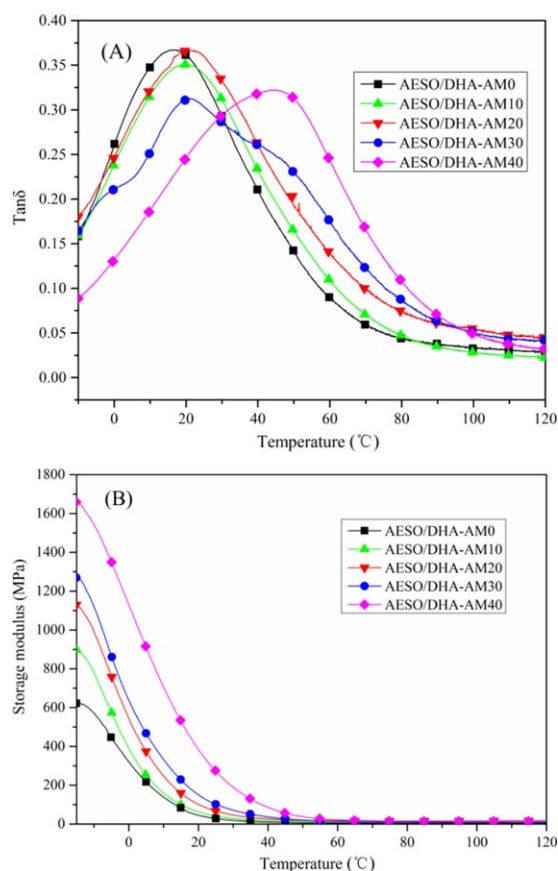


Figure 4. (A) $\tan \delta$ and (B) E' curves of the cured samples. [Color figure can be viewed at wileyonlinelibrary.com]

vibrations peak was not observed. Moreover, the characteristic absorption bands for the aromatic ring skeleton at approximately 1667 and 1534 cm^{-1} gradually increased in intensity because of the increase in the content of DHA-AM. These results imply that the reactants were completely copolymerized.

Dynamic Mechanical Properties of the Cured Samples

The dynamic mechanical properties of cured samples with different molar ratios are shown in Figure 4, and the data are summarized in Table II. As shown by the curves in Figure 4, similar DMA behaviors were found in this study. The peak of the loss tangent ($\tan \delta$) was single; this indicated that the cured samples were compatible and homogeneous.³⁵ The T_g of each cured sample was measured from the peak temperature of \tan

δ . As is known to all, T_g of a cured resin rests with the structure of the monomers and the crosslinking density of the cured samples. As the DHA-AM content increased, the T_g values of the cured samples became higher; this suggested that the addition of DHA-AM rendered the copolymer with a stronger rigid molecular structure than that of the single AESO polymer. These results were likely due to the large phenanthrene ring structure in DHA-AM rather than long aliphatic chains, which seemed to put more restriction on the chain segmental movement. On the other hand, the crosslinking density, which is discussed later, may have been another reason for the improved T_g values. The formation of AESO-rich and DHA-AM-rich regions with variable compositions in the polymer was a possible effect that resulted in a broad glass-transition behavior and spanned the range of the different phase transitions. As reported, interpenetrating polymer networks are a commonly used explanation for this behavior on the microlevel.¹⁶ Obviously, E' , which was also related to the chemical structure and crosslinked state, was strengthened significantly with increasing DHA-AM content. Clearly, the final E' was obtained from the AESO/DHA-AM40 sample. Nevertheless, the crosslinking density was conversely influenced by E' , which was considered to be equivalent to the elastic modulus in the rubbery plateau region. The experimental crosslinking density (ν_e) of the cured resins was calculated with the following equation^{31,36}:

$$E = 3\nu_e RT$$

where E is the elastic modulus of the crosslinked polymer, which can be considered to be equivalent to E' in the rubbery plateau region; R is the gas constant; and T is the temperature (K). To make sure the cured resins were in the rubbery state, the value of E' at $T_g + 40^\circ\text{C}$ was used to replace that of E . The data of the crosslinking density of the cured systems are shown in Table II.

Mechanical Properties of the Cured Samples

The mechanical properties of the cured samples were investigated. The compared results, including those of the crosslinking density, are listed in Table II, and the tensile stress–strain curves of the AESO/DHA-AM samples with different molar ratios are shown in Figure 5. We observed that the breaking elongation of the copolymers ranged from 24.7 to 36.1%, and the tensile strength changed from 1.1 to 5.7 MPa. The cured AESO/DHA-AM40 sample exhibited the highest tensile strength and breaking elongation, whereas the cured pure AESO showed the lowest tensile strength and breaking elongation. The result was

Table II. Analysis of the Mechanical and Thermal Properties of the Cured Samples

Sample	T_g ($^\circ\text{C}$)	E' at 25 $^\circ\text{C}$ (MPa)	Breaking elongation (%)	Tensile strength (MPa)	$T_{5\%}$ ($^\circ\text{C}$)	$T_{50\%}$ ($^\circ\text{C}$)	T_{\max} ($^\circ\text{C}$)	Crosslinking density (mol/m ³)
AESO/DHA-AM0	16	28	24.7 ± 0.3	1.1 ± 0.2	329.8	404.4	402.1	751
AESO/DHA-AM10	19	41	27.0 ± 0.1	1.6 ± 0.1	332.6	403.5	407.2	1531
AESO/DHA-AM20	20	67	27.4 ± 0.1	2.0 ± 0.1	331.5	406.0	409.5	1987
AESO/DHA-AM30	22	102	32.0 ± 0.3	4.3 ± 0.1	333.3	407.1	410.4	1616
AESO/DHA-AM40	45	273	36.1 ± 0.3	5.7 ± 0.2	335.6	408.8	411.6	1606

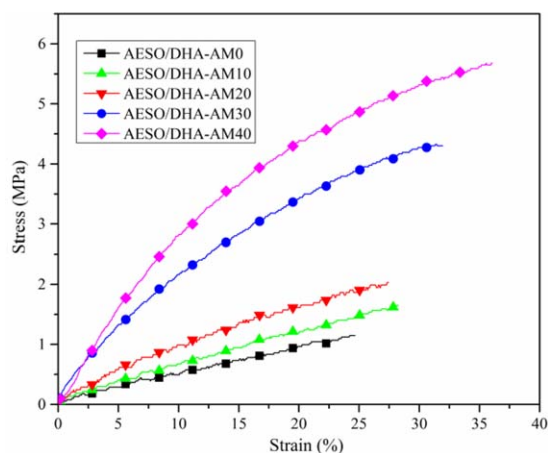


Figure 5. Tensile stress–strain curves of the cured samples. [Color figure can be viewed at wileyonlinelibrary.com]

indicative of improvements in the tensile strength and breaking elongation observed with the addition of DHA-AM.

With different molar ratios of the monomers, the chemical structures and crosslinked states in the cured resins varied accordingly and significantly.³⁶ The residual monomers in the copolymers served as plasticizers; meanwhile, DHA-AM was the hardening agent for the cured resins.³⁷ When a lower content of DHA-AM was added, the components in the cured system were mostly homopolymerized rather than copolymerized. Therefore, AESO/DHA-AM10 and AESO/DHA-AM20 had similar properties with to the cured AESO/DHA-AM0. Moreover, AESO/DHA-AM30 and AESO/DHA-AM40, with higher DHA-AM contents, showed significant improvement in both tensile strength and breaking elongation. The stronger tensile strength may have been due to the fact that the hydrogen bonds of N–H and the main crosslinking densities in the copolymer were enhanced with increasing DHA-AM. Moreover, a higher crosslinking density also bestowed with a higher breaking elongation. More narrowly, the visibly improved tensile strength of AESO/DHA-AM30 and AESO/DHA-AM40 could be explained by the synergistic effect of hydrogen bonding and crosslinking density.

TGA of the Cured Samples

Figure 6 shows different TGA curves for the samples. The 5%, 50%, and maximum weight loss temperatures ($T_{5\%}$, $T_{50\%}$, and T_{max} , respectively) are summarized in Table II. As we know, the initial weight loss temperature ($T_{5\%}$) is related to the decomposition of soluble or unreacted components. Obviously, we found that the $T_{5\%}$ values of all of the cured samples were higher than 329 °C; this revealed that the cured samples all had high thermal stabilities. In addition, $T_{50\%}$, which represents the main-chain degradation, was above 404 °C; this indicated the rigid structure in the polymer. Furthermore, T_{max} , which was the corresponding temperature at the maximum rate of weight loss, was also improved from 402.1 to 411.6 °C. These results demonstrate that the $T_{5\%}$, $T_{50\%}$, and T_{max} values in AESO/DHA-AM40 were all higher than those of the other samples. The decomposition of the unreacted components and the main-chain degradation were all improved slightly with DHA-AM because of the rigid

confined phenanthrene ring structure and the higher crosslinking density.³⁸ These results were indicative of improvements related to the high thermostability.

Elemental Analysis of the Cured Samples

To verify that AESO and DHA-AM were combined by chemical linking, a purification process was carried out for the AESO/DHA-AM samples before elemental analysis. The elemental analyses of the purified AESO/DHA-AM samples were performed, and the calculated results are listed in Table III. The mass fractions of nitrogen and carbon are represented by eqs. (1) and (2), respectively. C_1 and C_2 in the equations represent the molar quantities of DHA-AM and AESO in W grams of copolymer units, respectively. According to eqs. (1) and (2), the molar fraction of the DHA-AM monomer in the purified AESO/DHA-AM was derived with eq. (3). With increasing DHA-AM content, the nitrogen contents in the polymers increased. This phenomenon could be explained by the fact that the nitrogen element only existed in the DHA-AM monomer. Additionally, the changes in the calculated elemental content were basically in accordance with the theoretical values. The results indicate that DHA-AM was copolymerized with AESO in the system:³⁹

$$N\% = \frac{14C_1}{W} \quad (1)$$

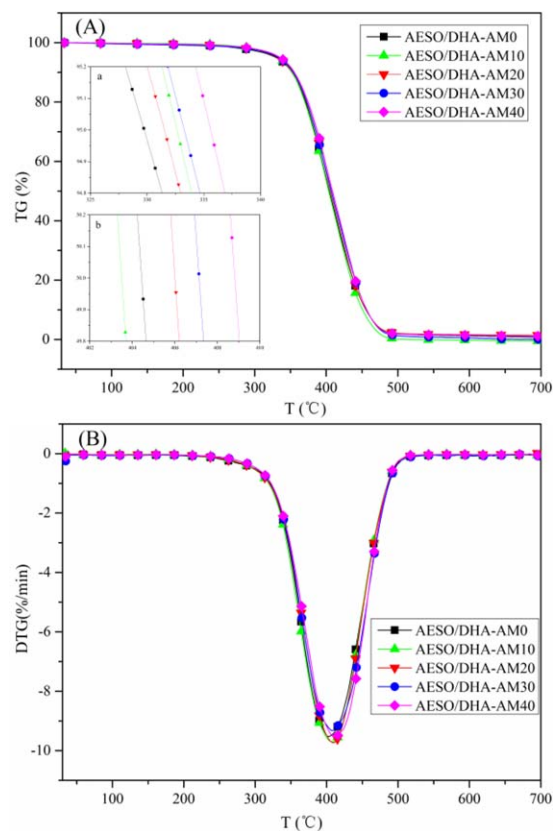


Figure 6. (A) Thermogravimetry (TG) and (B) derivative thermogravimetry (DTG) curves for the different cured samples. [Color figure can be viewed at wileyonlinelibrary.com]

Table III. Elemental Analysis of the Purified AESO/DHA-AM Samples

Sample	C (wt %)		H (wt %)		N (wt %)		DHA-AM (mol %)	
	Found	Calcd	Found	Calcd	Found	Calcd	Found	Calcd
AESO/DHA-AM0	68.2	67.5	9.72	9.64	0	0	0	0
AESO/DHA-AM10	68.6	68.0	9.72	9.71	0.138	0.0629	10	4.77
AESO/DHA-AM20	69.2	68.3	9.72	9.71	0.297	0.214	20	15.1
AESO/DHA-AM30	69.8	68.6	9.72	9.35	0.485	0.291	30	19.7
AESO/DHA-AM40	70.5	69.3	9.72	9.65	0.709	0.538	40	32.8

$$C\% = \frac{12(23C_1 + 62C_2)}{W} \quad (2)$$

$$\frac{C_1}{C_1 + C_2} = \frac{372N\%}{234N\% + 7C\%} \quad (3)$$

θ Analysis of the Cured Samples

The θ diagrams of the cured samples are shown in Figure 7. The pure cured sample without DHA-AM was found to be a hydrophilic material with a θ of 81°. For AESO/DHA-AM10, AESO/DHA-AM20, AESO/DHA-AM30, and AESO/DHA-AM40, the measured θs were 91, 95, 102, and 105°, respectively. All of the copolymers exhibited hydrophobic characteristics, and the AESO/DHA-AM40 sample showed the highest θ value because the largest molar proportion of DHA-AM was added to this sample. The large phenanthrene ring structure of DHA-AM was responsible for their hydrophobicities. Moreover, the water resistance was enhanced by the addition of DHA-AM, which changed the interfacial energy of the cured resin.

CONCLUSIONS

DHA-AM, a rosin-based polymeric monomer, was synthesized and introduced into an AESO/DHA-AM system to afford a thermosetting resin by thermocuring. The large phenanthrene ring structure in DHA-AM contributed more restriction to the chain segmental movement than long aliphatic chains. When the content of DHA-AM in the copolymer was increased from 0 to 40% (molar ratio), the cured samples exhibited increasing E , T_g , and thermal stability values. The hydrogen bonds of N—H and main crosslinking densities in the copolymer enhanced the tensile strength with increasing DHA-AM molar ratio. The large phenanthrene ring structure with hydrophobic

characteristics changed the copolymers from hydrophilic to hydrophobic materials. In conclusion, the DHA-AM monomer, with its large phenanthrene ring structure and hydrogen-bonding interactions, copolymerized with AESO will be useful in the development of heat-resistant and hydrophobic materials.

ACKNOWLEDGMENTS

The authors express their gratitude for the financial support of the National Natural Science Foundation of China (contract grant number 31470597) and the Central Special Foundation for Basic Research in the Public Interest of the Chinese Academic of Forestry (contract grant number CAFINT2014C07).

REFERENCES

- Mustata, F.; Tudorachi, N.; Rosu, D. *Compos. B* **2011**, *42*, 1803.
- Biermann, U.; Bornscheuer, U.; Meier, M. A.; Metzger, J. O.; Schäfer, H. *J. Angew. Chem. Int. Ed.* **2011**, *50*, 3854.
- Huang, X.; Liu, H.; Shang, S.; Rao, X.; Song, J. *J. Agric. Food Chem.* **2015**, *63*, 9062.
- Suman, M.; La Tegola, S.; Catellani, D.; Bersellini, U. *J. Agric. Food Chem.* **2005**, *53*, 9879.
- Webster, D. C.; Sengupta, P. P.; Chen, Z.; Pan, X.; Paramarta, A. U.S. Pat. 9,096,773 (2015).
- Adhvaryu, A.; Erhan, S. *Ind. Crops Prod.* **2002**, *15*, 247.
- Gu, H.; Ren, K.; Martin, D.; Marino, T.; Neckers, D. C. *J. Coat. Technol.* **2002**, *74*, 49.
- Bajpai, M.; Shukla, V.; Singh, D.; Singh, M.; Shukla, R. *Pigment Resin Technol.* **2004**, *33*, 160.
- Liu, Z.; Erhan, S. Z.; Xu, J. *Polymer* **2005**, *46*, 10119.
- Lee, S.-H.; Lee, S.-Y.; Lim, H.-K.; Nam, J.-D.; Kye, H.-S.; Lee, Y.-K. *Polym. Korea* **2006**, *30*, 202.
- Zhan, M.; Wool, R. P. *J. Appl. Polym. Sci.* **2010**, *118*, 3274.
- La Scala, J.; Wool, R. P. *Polymer* **2005**, *46*, 61.
- Khot, S. N.; Lascalea, J. J.; Can, E.; Morye, S. S.; Williams, G. I.; Palmese, G. R.; Küsefoğlu, S. H.; Wool, R. P. *J. Appl. Polym. Sci.* **2001**, *82*, 703.
- Grishchuk, S.; Karger-Kocsis, J. *Express Polym. Lett.* **2011**, *5*, 2.

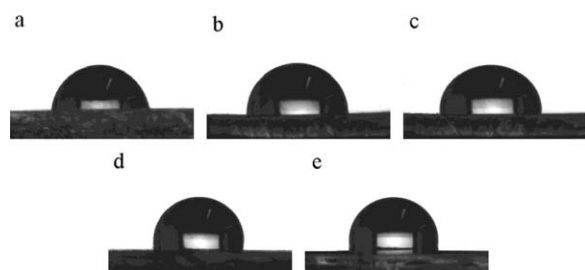


Figure 7. θs of the cured samples: (a) AESO/DHA-AM0 (81°), (b) AESO/DHA-AM10 (91°), (c) AESO/DHA-AM20 (95°), (d) AESO/DHA-AM (102°), and (e) AESO/DHA-AM (105°).

15. Lu, J.; Khot, S.; Wool, R. P. *Polymer* **2005**, *46*, 71.
16. Can, E.; Wool, R.; Küsefoğlu, S. *J. Appl. Polym. Sci.* **2006**, *102*, 1497.
17. Kundu, P. P.; Larock, R. C. *Biomacromolecules* **2005**, *6*, 797.
18. Li, F.; Hanson, M.; Larock, R. *Polymer* **2001**, *42*, 1567.
19. Lu, Y.; Larock, R. C. *J. Appl. Polym. Sci.* **2006**, *102*, 3345.
20. Lu, Y.; Larock, R. C. *Biomacromolecules* **2006**, *7*, 2692.
21. Andjelkovic, D. D.; Larock, R. C. *Biomacromolecules* **2006**, *7*, 927.
22. Campanella, A.; Scala, J. J. L.; Wool, R. *J. Appl. Polym. Sci.* **2011**, *119*, 1000.
23. Fertier, L.; Koleilat, H.; Stemmelen, M.; Giani, O.; Joly-Duhamel, C.; Lapinte, V.; Robin, J.-J. *Prog. Polym. Sci.* **2013**, *38*, 932.
24. Dong, Y.; Yan, Y.; Wang, K.; Li, J.; Zhang, S.; Xia, C.; Shi, S. Q.; Cai, L. *Eur. J. Wood Wood Prod.* **2016**, *74*, 177.
25. Liu, X.; Huang, W.; Jiang, Y.; Zhu, J.; Zhang, C. *Express Polym. Lett.* **2012**, *6*, 293.
26. Mustata, F. R.; Tudorachi, N. *Ind. Eng. Chem. Res.* **2010**, *49*, 12414.
27. Yao, F.; Zhang, D.; Zhang, C.; Yang, W.; Deng, J. *Bioresour. Technol.* **2013**, *129*, 58.
28. Liu, X.; Xin, W.; Zhang, J. *Bioresour. Technol.* **2010**, *101*, 2520.
29. Kim, S. J.; Kim, B. J.; Jang, D. W.; Kim, S. H.; Park, S. Y.; Lee, J. H.; Lee, S. D.; Choi, D. H. *J. Appl. Polym. Sci.* **2001**, *79*, 687.
30. Ray, S. S.; Kundu, A.; Ghosh, M.; Maiti, S. *Eur. Polym. J.* **1985**, *21*, 131.
31. Ma, Q.; Liu, X.; Zhang, R.; Zhu, J.; Jiang, Y. *Green Chem.* **2013**, *15*, 1300.
32. Ma, S.; Li, T.; Liu, X.; Zhu, J. *Polym. Int.* **2016**, *65*, 164.
33. Yang, Y.; Shen, M.; Liu, H.; Shang, S.; Song, Z. *Biomass Chem. Eng.* **2016**, *50*, 6.
34. Tao, Z.; Yang, S.; Chen, J.; Fan, L. *Eur. Polym. J.* **2007**, *43*, 1470.
35. Reddy, T. T.; Hadano, M.; Takahara, A. *Macromol. Symp.* **2006**, *242*, 241.
36. Yang, X.; Li, S.; Xia, J.; Song, J.; Huang, K.; Li, M. *Ind. Crops Prod.* **2015**, *63*, 17.
37. Henna, P.; Larock, R. C. *J. Appl. Polym. Sci.* **2009**, *112*, 1788.
38. Huang, Y.; Pang, L.; Wang, H.; Zhong, R.; Zeng, Z.; Yang, J. *Prog. Org. Coat.* **2013**, *76*, 654.
39. McCormick, C. L.; Chen, G. S.; Hutchinson, B. H. *J. Appl. Polym. Sci.* **1982**, *27*, 3103.